



BTEXS Removal From Aqueous Phase by MCM-41 Green Synthesis Using Rice Husk Silica

M. Heydari¹, T. Tabatabaie^{1*}, F. Amiri¹, S. E. Hashemi^{1,2}

¹ Department of Environment, Bushehr Branch, Islamic Azad University, Bushehr, Iran

² Department of Environmental Health Engineering, Faculty of Health and Nutrition, Bushehr University of Medical Sciences, Bushehr, Iran

P A P E R I N F O

Paper history:

Received 03 February 2023

Accepted in revised form 27 March 2023

Keywords:

Adsorption
 BTEXS aromatics
 MCM-41 catalyst
 Rice husk ash
 Taguchi method

A B S T R A C T

Large volumes of contaminated industrial wastewater have caused growing concern among researchers and environmentalists. Benzene, toluene, ethylbenzene, xylene, and styrene (BTEXS) cyclic hydrocarbons in industrial effluents are often completely stable to biodegradation and must be treated before disposal. In this context, using adsorption processes is a potential alternative for treating a wide range of organic pollutants, especially aromatic compounds in industrial wastewater. This study investigated the preparation of MCM-41 from silica; extracted from rice husk ash; MCM-41 was green synthesized to evaluate the effect of mesoporous used in BTEXS removal of an aqueous medium using the Taguchi method. The aqueous solution contains cyclic hydrocarbons was synthetically prepared based on real industrial effluent in concentrations of 50, 100, and 150 mg/l using MCM-41 catalysts, in doses of 0.1, 0.5, and 1g, at different pH values. In the present study, the optimum results obtained by Taguchi method analysis were pH =11, for duration of 60 minutes, the concentration of cyclic hydrocarbon solution BTEXS 100 mg/l, and nanoparticle dose of 0.5 g. The maximum BTEXS removal of 77.36% was achieved by the use of hydrogen peroxide.

doi: 10.5829/ijee.2023.14.04.02

INTRODUCTION

Pollutants from activities that are harmful to human health and can pose a serious threat to all organisms as well as detrimental effects on the environment are currently a significant concern in petroleum industry [1]. The separation of petroleum products from water has become the focus of global attention for wastewater treatment. Process water leakage and discharge of water contaminated with cyclic hydrocarbons into groundwater aquifers caused serious damage and created environmental hazards. Chronic exposure to these contaminants can cause various diseases. It can also negatively affect ecosystems and aquatic species due to the proximity of the processing unit to the sea. The treatment processes are generally a challenge for industrial production because of containing metals, heavy oil, petroleum sludge, and other pollutants [2]. The complexity of these systems requires compliance with

specific working conditions, and technical training, equipment, methodologies, and standards [3]. BTEX is a challenging group of volatile organic compounds in an industrial area [4-6]. Moreover, styrene monomer one of the most well-known aromatic volatile organic compounds [7] produced from petrochemicals affects workers' health [8]. Aromatic hydrocarbons are toxic compounds, which have negative effects on the skin, respiratory and nervous systems, and even carcinogens [9-11]. Different techniques and processes have been used to treat benzene and toluene-contaminated water and usually show different levels of success. Currently, conventional treatments include filtration [12], distillation [13], evaporation [14], reverse osmosis [15], and coagulation [16]. Although these techniques are particularly effective, some associated disadvantages such as high operating and maintenance costs and by-product (such as toxic sludge), encourage researchers to find alternative therapies [17, 18]. In recent years, special

*Corresponding Author Email: Tayebeh.Tabatabaie@iau.ac.ir
 (T. Tabatabaie)

attention has been paid to adsorption processes, which is mainly due to some attractive features such as simplicity of work, low cost, and the absence of secondary pollution hazards [19-22].

In the early 1990s, scientists at Mobil Oil Corporation synthesized the first ordered mesoporous silicate materials known as the M41S family [23]. M41S is the general term used to describe the various types of Mobil Composition of Matter (MCM) synthesized at primary conditions in the presence of alkyl ammonium surfactants and silica sources whose pore sizes are 3-10 nm in diameter. Mesoporous MCM-41 is the best-known type of this substance [24-26]. This has wide application in organic synthesis and was used in several types of reactions due to their diversity [27]. Today, a cheap silica source is used to synthesize MCM-41. Despite ensuring sustainable food security, the rice milling process produces the residual biomass of about 120 million tons per year of rice husk (RH) [28], which can act as significant feedstock storage for the activated silica in MCM-41 synthesis [29, 30]. In most developing countries, RH is often discarded in palatable water and left untreated in a landfill. Due to the fermentation of RH by microorganisms, these unethical activities pollute water and produce greenhouse gases (GHGs). Alternatively, only a small number of rice mills use incineration/on-site burning or open burning, which can cause severe air pollution and environmental problems [31]31[32]. Rice husk ash (RHA) has distinct pozzolanic properties, meaning it provides reactive SiO₂ to react with water during the process [33].

The efficient treatment of cyclic hydrocarbons is of considerable importance and has attracted much attention. In recent years; many articles have been published on the removal of cyclic hydrocarbons using adsorbent like MCM-41 catalyst. For example, organic vapors [34], sorbent of thiophene [35], toluene degradation [36], catalytic ozonation of toluene [37], reaction-type adsorption of o-xylene [38], volatile organic compounds [39], selective oxidation of styrene into benzaldehyde [40], and o-xylene removal from gas streams [41].

To minimize the number of require experiments, and maximize results effectiveness, some efficient schemes, such as fractional factorial schemes help identify essential factors and generate functional initial experiments [42, 43]. The orthogonal design and the Taguchi method are two common types of fractional factorial design matrices [44], where the latter ones used significantly in industrial countries [45-47], as a simple and effective way to improve products and increase process quality to reduce the number of experimental combinations. Compared to the orthogonal design, signal-to-noise ratio (S/N) was introduced in the Taguchi method to determine the quality of product characteristics in terms of product response to noise factors and signal factors [48, 49]. Since it requires a

minimum number of experimental tests, and its conclusions are statistically reliable, this method is both cost-effective and efficient [43].

The purpose of present research is to synthesize an active catalyst like MCM-41 by using rice husk silica as adsorbent for the removal of BTEXS in aqueous phase. Adsorption experiments were performed using the Taguchi method. Elimination experiments were performed in a double-walled reactor at a constant temperature. The effect of using hydrogen peroxide an aqueous solution containing cyclic hydrocarbons was tested. The reuse of MCM-41 catalyst in an aqueous solution containing BTEXS cyclic hydrocarbons was investigated and analyzed.

MATERIALS AND METHODS

Materials

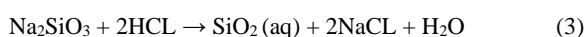
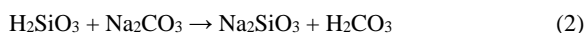
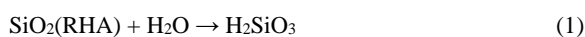
Hydrochloric acid and absolute ethanol supplied by Merck (Germany). Methanol withpurity of 99% was supplied by Zagrou petrochemical company. N-Cetyl-N, N, NTrimethylammonium Bromide (CTAB), and hydrogen peroxide (32%) obtained from Merck. Benzene, Toluene and O-xylene supplied by Nouri petrochemical company (Iran); Ethylbenzene and Styrene monomer (99.9%) provided by Pars petrochemical company (Iran). Sodium iodide (99.5%), Sodium thiosulfate (97.0%) and Sodium hydroxide (99%) supplied by Merck. Rice husk was purchased from Sabs Golbaran company and was packaged from local farms (Rasht, Iran). All chemicals purchased from companies in this study were used without further purification. Distilled water was used in all stages of solution preparation.

Extraction of silica from rice husk

According to previous research, pure silica was extracted from rice husks with minor modifications [50]. Thus, the first 30 g of purchased rice husk was first washed with distilled water to remove the dust sitting on it completely. This was then rinsed with 1 N hydrochloric acid and calcined and converted to ash at 550 °C for one hour. 5 g of ash with 50 ml of deionized water, with a constant ratio of 1 to 10 is added until 5 g is utterly mixed in 50 ml of water. An ultrasonic device with a frequency of 40 Hz, is used to place in water for 5 minutes to get uniform ash distribution. It was then mixed with 1 N sodium carbonate in equal volumes from the previous step and stirred for 2 hours at 90 °C by alternating stirrer. The solution was then cooled to room temperature and centrifuged for 15 minutes at 4650 rpm. The supernatant, carbonic acid, was stored as needed for further reduction and study, and the residue was neutralized with 1 N hydrochloric acid. The resulting residue was washed several times with distilled water. As follow 50 ml of distilled water was used during four steps, and after each

washing step, the solution was converted into two phases. The liquid surface solution was drained, and the next washing step was performed again on the sediment. This was then exposed to the open air for two days to dry the sample. Finally, the model was placed in an oven at 80 °C for 3 hours to dry completely.

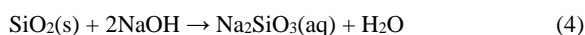
The equations for converting rice husk ash to silica are given below (Equations (1)-(3)), [50].



Final tests of silica extracted from rice husk, including XRF, XRD, and FTIR were performed to ensure the presence of silica in the sample.

Conversion of silica extracted from rice husk to sodium silicate solution

To prepare sodium silicate, according to previous research [40, 51] and some changes in the procedure firstly, 0.57 g of the extracted silica was added to 10 ml of 1 N sodium in a 10 ml flask and allowed to mix and become uniform. Stir well for 1 hour at 80 °C. The solution was then stirred continuously for 23 hours at room temperature. Later on, it was filtered with a filter syringe head. It was washed with 20 ml of distilled water, and finally, a clear solution of sodium silicate was obtained, according to the following formula (Equation (4)).



Sodium silicate extracted from rice husk was added dropwise to the mixture in a specified amount for each synthesis stage according to the instructions.

Synthesis of MCM-41 catalyst

The synthesis of MCM-41 was performed with modifications according to previous research work presented by Cai et al. [52]. 0.28 g of NaOH was dissolved in 487 g of deionized water. This stirring continued to some extent until the NaOH pellet was wholly dissolved in deionized water. 1 g of CTAB surfactant was weighed and added to solution A at 80 °C to be mixed. This stirring was continued for one hour until a homogeneous solution was obtained. At this stage, 5 ml of silica source extracted from rice husk (solution made from the previous step) was added slowly and dropwise to the homogeneous solution obtained. The solution was stirred for 2 hours at 80°C. Erlenmeyer from the final solution was placed in a stationary place for 24 hours after finishing the work so that the obtained sediment was almost wholly settled. Then, using a centrifuge for 15 minutes and 4650 rpm, was remove the resulting residue, and placed in the open air for three days until the sample is dry.

To remove surfactants and impurities, the dried sample obtained from the previous step was placed in an electric furnace with a temperature of 550 degrees Celsius to heat up and a pure sample was obtained. By calcination, the organic compounds were blackened and removed from the catalyst structure, leaving the pure white compound of the MCM-41 catalyst.

Analytical methods

The surface areas and pore size distributions of the produced silica were determined by Brunauer–Emmett–Teller (BET) and Barrett Joyner–Halenda (BJH) methods, (Manufacturer: BEL, Device model: BELSORP MINI II, and Country of manufacture: Japan). The chemical composition of each sample was determined by XRF using an energy-dispersive X-ray spectrometer, (Manufacturer: PHILIPS, Device model: PW1410, and Country of manufacture: Netherlands). Phase formation and crystallographic state of all models were analyzed using XRD analysis using an X-ray diffraction gauge, (Manufacturer: Philips, Device model: PW1730, and Country of manufacture: Netherlands), and CuK α as source ($\lambda = 1.54056$). Samples were scanned in the range of $2\theta = 10$ -80 degrees at a speed of 2 degrees per minute. The morphology of the samples was examined using a field emission scanning electron microscope, (Manufacturer: TESCAN, Device model: MIRA III, (Czech Republic), equipped with an accelerator voltage of 15 kV. The pieces were first placed in a vacuum chamber and covered with a thin layer of gold (Au). Transmission electron microscope images of the pieces were obtained using a transmission electron microscope, (Device model: CM120, and Country of manufacture: Netherlands), operating at a voltage of 100 kV. Samples were first prepared by dispersing the particles in ethanol and loading them onto a Formvar-coated copper mesh. To identify the presence of a catalyst used in the solution and to contaminate the existing materials used to make the catalyst, experiments were performed at a wavelength of 200 to 800 nm by a single-beam UV/Visible device, (Varian, Device model: CARY50, Australia). The density of the aqueous solution containing cyclic hydrocarbons was measured using densitometer (ANTON PAAR, Device model: DMA 4500, Australia).

Procedures for catalytic tests

After weighing the MCM-41 catalyst in different quantities tested, a purchased tea filter bag was used to hold the catalyst in an aqueous solution containing cyclic hydrocarbons (Figure 1). For this stage of the research, the solution was concentrated in methanol in a 20 ml vial with code. This concentrated solution was stored in the refrigerator until the end of the research experiments. Dilute solutions of 50, 100, and 150 mg/l were made separately from the concentrated solution in a 100 ml flask containing distilled water. This standard solution was performed by Taguchi experiments to evaluate the

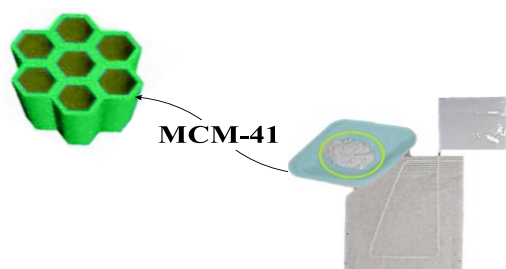


Figure 1. Example of a tea filter bag containing MCM-41 catalyst

synthesized sample of MCM-41 catalyst with doses (0.1, 0.5, and 1.0) g; time (30, 60, and 90) minutes and pH (3, 7, and 11). In this work, four effective factors, including reaction time, initial concentration of cyclic hydrocarbons (BTEXS), catalyst dose, and pH, are considered in 3 levels each. Table 1 summarized the studied factors with their related levels. According to the Taguchi software model for each test, the variables and their levels were proposed according to the L9 array with nine experiments, and the experiments were performed under the same conditions.

The sampling stage was performed through a 10 ml sampler. In addition, at each stage of selection, a new sampler was used to remove contamination of the aqueous solution containing cyclic hydrocarbons. An aqueous solution containing BTEXS cyclic hydrocarbons was made in a 100 ml flask, and the total concentrations of cyclic hydrocarbons 250, 500, and 750 mg/kg were selected. All experiments were performed in a double-walled reactor connected to the chiller at 24 °C.

Catalytic tests for removing BTEXS

Based on the adapted ISO 11423 Method [53], BTEXS analysis was performed at the end of the experiment and sampling with a 10 ml sampler in special vials. According to previous research [40], Changes were made in the device conditions for the analysis of cyclic hydrocarbons. A Poly Ethylene Glycol column (CP-WAX 30 m, 0.32 mm id, 0.5 μm thickness) was used for BTEXS analysis. The initial column temperature was 55 °C for 10 min. Then, the temperature was increased to 150 °C at a rate of 10 °C.min⁻¹. The injector temperature

Table 1. Parameters and test levels of MCM-41 catalyst

No.	Parameter	Levels		
		Level 1	Level 2	Level 3
1	pH	3	7	11
2	Time (minutes)	30	60	90
3	The concentration of cyclic hydrocarbon (mg/kg)	50	100	150
4	MCM-41 catalyst dose change (g)	0.1	0.5	1.0

was 220 °C. The detector temperature was 240 °C with nitrogen as a carrier gas at 7 psig. The flame ionization detector was also used using synthetic air (300 mL min⁻¹), hydrogen (30 mL min⁻¹), and nitrogen makeup (25 mL min⁻¹). The injection volume was 1.0 ml. The temperature of the headspace system was 70 °C for 60 min.

To measure the values of COD and TOC in this study, a 2400 model spectrophotometer was tested at the beginning and end of the test from an aqueous solution containing cyclic hydrocarbons. It should be noted that for experiments, special reagents for COD and TOC testing in different ranges (LR, MR, and HR ranges) from HACH company were used. Also, the HACH DRB200 reactor was used to heat the special COD and TOC vials.

Removal of BTEXS using MCM-41 catalyst in the presence of H₂O₂

Hydrogen peroxide is considered an energy and safety carrier and environmentally friendly oxidant that is widely used in biological sciences, medicine, and environmental remediation [54]. At this stage of the experiment, the highest and lowest point of removal of BTEXS cyclic hydrocarbons an aqueous solution obtained by the Taguchi method was investigated. According to previous research [3], a concentration of 0.1 M of hydrogen peroxide was selected for this study.

Numerous methods have been mentioned in recent research [55] to track consumed peroxide. However, due to the nature of the sample in this study and also the high cost of raw materials to perform hydrogen peroxide testing with previous methods, it is not economical, and besides, they have a test error. In this study, to correct the mentioned cases, it was suggested to perform a hydrogen peroxide test in an aqueous solution containing cyclic hydrocarbons using ASTM D-2340 [56]. To do this, 25 ml of isopropyl alcohol was added to two 500 ml Erlenmeyer flasks, each containing several boiling stones and then 1 ml of glacial acetic acid was added to the Erlenmeyer flasks. In one of the Erlenmeyer flasks was added 5 ml of an aqueous solution containing cyclic hydrocarbons and hydrogen peroxide. This Erlenmeyer was considered a sample and the second Erlenmeyer as a control. Mount the condenser and set the temperature to 20 °C. Heat the Erlenmeyer flask to boiling point and then add 5 ml of the NAI solution in isopropyl alcohol to each flask from the top of the condenser. The boiling was continued for 10 minutes, and after the end of the boiling step, the flasks were removed from the heater and 10 ml of distilled water was added to each condenser for washing. The flasks were cooled to room temperature, and the iodine released in each flask was titrated with Na₂S₂O₃ solution until the yellow color of the solution disappeared, and the sodium thiosulfate dose was recorded as 0.01 N.

The following formula was used to calculate the final results (Equation (5)):

$$x \frac{mg}{kg} H_2O_2 = \frac{(A-B)*N*1.7*10000}{g_{Sample} * C} \quad (5)$$

A: sodium thiosulfate consumed for sample (ml).

B: sodium thiosulfate for blank (ml).

N: Thiosulfate sodium normality (0.01 N).

C: Density of aqueous solution containing BTEXS cyclic hydrocarbons at 24 °C.

Reusability of MCM-41 Catalyst

An essential characteristic of a catalyst is its ability to be reused and stable. These properties were investigated and tested in the synthesis of the MCM-41 catalyst. Based on previous studies [57], and with the changes made in it, MCM-41 catalyst regeneration was performed. Because methanol is a cheap solvent and it is also a suitable solvent for solving the aqueous and organic phases. Methanol was used in this study instead of ethanol an expensive substance used in previous studies. The changes made in this study to regenerate the MCM-41 catalyst include the following: In the first stage, the MCM-41 catalyst was weighed in a tea filter bag before being added and packaged. The initial weight of 0.5001 g was removed from the MCM-41 catalyst and embedded in a filter. After completion and adsorption of hydrocarbons by the MCM-41 catalyst, the catalyst was removed from an aqueous solution containing BTEXS cyclic hydrocarbons and placed in a 60 ml vial containing 25 ml of methanol. The reason for choosing a wash with a selected volume of 25 ml of methanol is that the tea filter bag is wholly immersed in methanol.

Each washing step, which includes three steps until the end of the complete removal of hydrocarbons, was performed by an ultrasonic device of the ELMA model with a frequency of 40 Hz at a temperature of 35 °C, and each step was performed for 25 minutes. At each stage of leaching methanol and leaching methanol containing hydrocarbons extracted from the catalyst, the adsorption values were analyzed. After washing, the filter containing the MCM-41 catalyst was removed from the vial and rinsed with distilled water, and dried in the open air for 24 hours. Then the contents of the filter were removed and poured on the watch glass and kept in the oven at 200 °C for one hour. The reason for choosing a temperature of 200 °C is that if there is any hydrocarbon left, it will be destroyed entirely and evacuated at this temperature. Because the last welding temperature of the five selected cyclic hydrocarbon materials is 170 °C, 30 °C was also chosen higher.

RESULTS AND DISCUSSION

Characterization of silica from rice husk

FTIR analysis

The silica obtained from this study had bands approximately similar to commercial-grade silica, as

shown in Figure 2. The silanol (Si-O-H) and siloxane (Si-O-Si) groups were covered with no other impurity bands between 1630 and 3442 cm^{-1} . The obtained results confirm the research results [50, 58]. The band at 3442 is attributed to the stretching vibration of the O-H group, whereas the band position at 1630 cm^{-1} is attributed to the bending vibration of the H₂O molecule in the Si-OH group. The band at 1090 cm^{-1} is denoted by the asymmetric stretching vibration of Si-O-Si. The wavenumber at 798 cm^{-1} is arisen due to the symmetric stretching vibration of the Si-O bond while a band at 463 cm^{-1} is designated for the Si-O bending of the siloxane group [50, 59].

XRD analysis

Figure 3 shows the XRD pattern of the extracted silica. A broad hump at a $2\theta = 22^\circ$ was observed for silica, indicating the amorphous nature of the sample. In addition, at other scan angles from 10° to 80° , no other sharp peaks were observed, indicating the absence of a regular crystal structure. Irregular particle geometry also shows a high proportion of silica. This result proves that typical amorphous components existed in the absence of any stable crystalline phase. The obtained results confirm the research results [50, 51, 60].

XRF analysis

An XRF analysis of (Table 2) shows that siliceous sediments are primarily composed of SiO₂, with very few metal impurities.

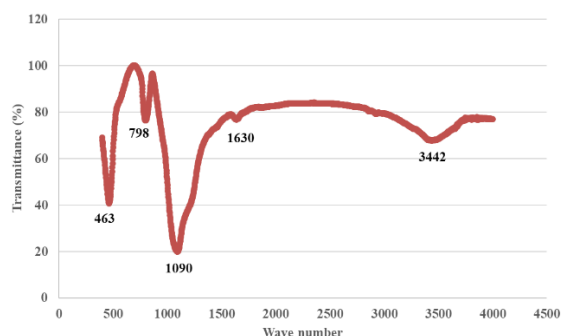


Figure 2. FTIR test of silica extracted from rice husk

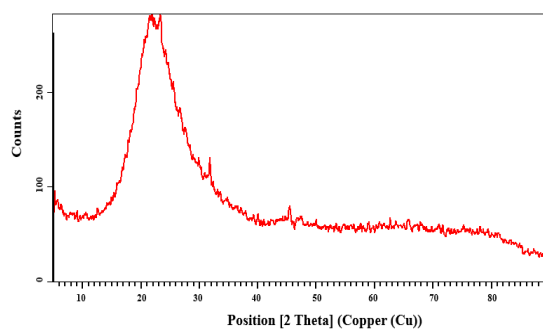


Figure 3. XRD test of silica extracted from rice husk

Table 2. Chemical composition properties of processed rice husk ash

Chemical properties	Rice husk ash (%)	Chemical properties	Rice husk ash (ppm)
SiO ₂	97.512	S	151
Al ₂ O ₃	0.093	Cl	988
Fe ₂ O ₃	0.033	Cr	6
CaO	0.63	Cu	36
MgO	0.49	Ni	34
Na ₂ O	0.457	Sr	46
K ₂ O	0.303	V	14
TiO ₂	0.032	Zn	152
Mno	0.112	Zr	1
P ₂ O ₅	0.171	Ce	57
LOI*	0	La	12

* LOI: loss on ignition

Characterization of MCM-41 catalysts

XRD analysis

To evaluate the crystallinity and structure of the synthesized MCM-41 catalyst, X-ray diffraction analysis was used. Figure 4 illustrated the high angel XRD trend of the synthesized MCM-41 catalyst. The characteristic peaks of MCM-41, at $2\theta = 22.51^\circ$ corresponding to (200) Miller indices, which are commonly used to identify MCM-41 catalyst from this region. We can see the peak that marks the plates forming the typical hexagonal material of the MCM-41 type. This indicates that the MCM-41 catalyst with a hexagonal structure has been synthesized correctly. The results obtained are consistent with the results [61].

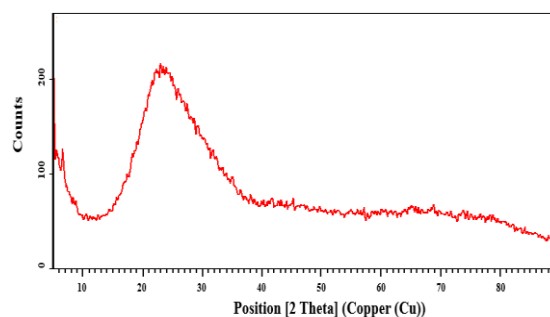


Figure 4. XRD test of MCM-41 catalyst synthesized from rice husk

BET analysis

After adsorption/desorption of N₂, a type-A hysteresis ring was formed for MCM-41 (Figure 5). The residual ring observed for the MCM-41 catalyst contained a berry gradient in adsorption and desorption, indicating that the pores were created by two parallel plates. Considering (Table 3), it is clear that the MCM-41 catalyst has a practically large surface area. The structural data of the MCM-41 catalyst nanoparticles are summarized in (Table 3). The obtained results confirm the results of the research [62].

SEM analysis

The morphology of the synthesized catalyst was investigated using a field diffusion scanning electron microscope. (Figure 6) shows the SEM image of the

Table 3. Summary of BET and BJH plots

Composition name	Total pore	Mean pore diameter (nm)	as, BET (m ² /g)	V _m (cm ³ (STP)/g)
	Volume (cm ³ /g)			
MCM-41	1.0616	5.7474	738.82	169.75

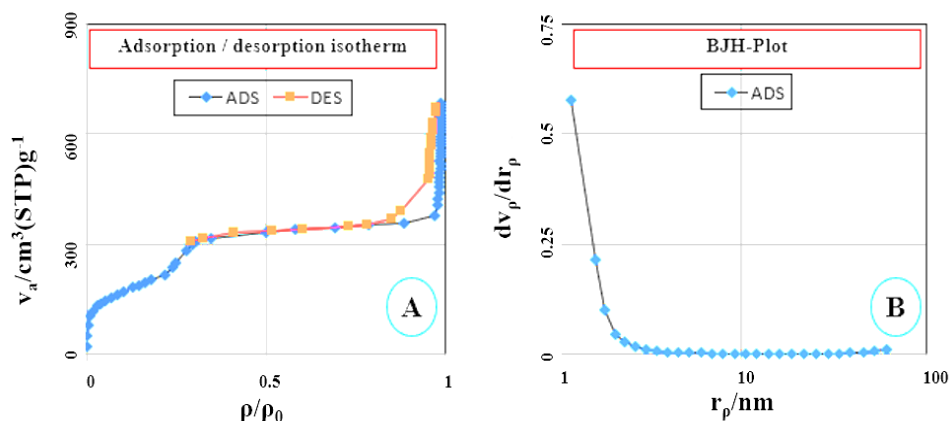


Figure 5. (A) Adsorption/desorption N₂ isotherms and (B) pore size distribution of MCM-41

MCM-41 catalyst. Using the synthesized MCM-41, it was determined that its morphology is uniform and spherical. The obtained results confirm the results of the research [63].

TEM analysis

The MCM-41 Transmission Electron Microscope (TEM) image is shown in Figure 7. The elliptical particles confirm the MCM-41 catalyst. This shape is usually the distinction between mesoporous and hexagonal pores, which is related to the MCM-41 catalyst. The obtained results confirm the results of the research [64].

MCM-41 catalytic activity

In this study, to reduce or eliminate errors, each sample was made twice based on the Taguchi L9 array and tested in each step. For this purpose, we have nine experiments for each step, each experiment was repeated twice, and a total of 18 experiments were performed for each synthesis step.

Removal of cyclic hydrocarbons using MCM-41 catalyst

In the first step, the solution was concentrated in methanol in a 20 ml vial. This concentrated solution was

stored in the refrigerator until the end of the research experiments. Before adding the MCM-41 catalyst to 100 ml balloons, standard samples made at three concentrations of 50, 100, and 150 mg/kg were first analyzed. Considering the bias values in the table above, which is less than 5%, the results showed that the standard sample made using theoretical calculations and the output of the chromatographic device is the same.

Preliminary COD and TOC tests were performed before adding the MCM-41 catalyst to the standard sample. The values obtained are given in the tables below. The mean value for the next calculations was considered for the COD and TOC tests and the ratio of the two. The (Equation (6)) was used to determination of removal efficiency [65]:

$$RE (\%) = \frac{(C_0 - C)}{C_0} * 100 \quad (6)$$

Results of MCM-41 catalyst samples based on Taguchi experiments

- Results design of experiment

By applying the Taguchi method, the variability can be shown at the signal-to-noise ratio. The highest S/N ratio

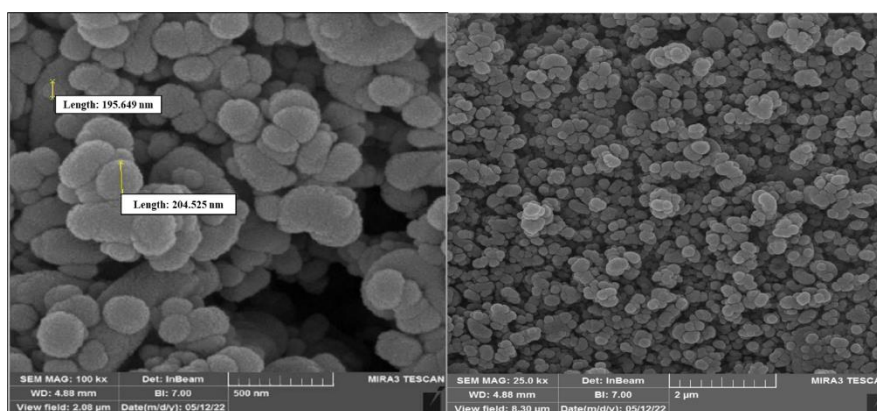


Figure 6. SEM images of MCM-41 catalyst

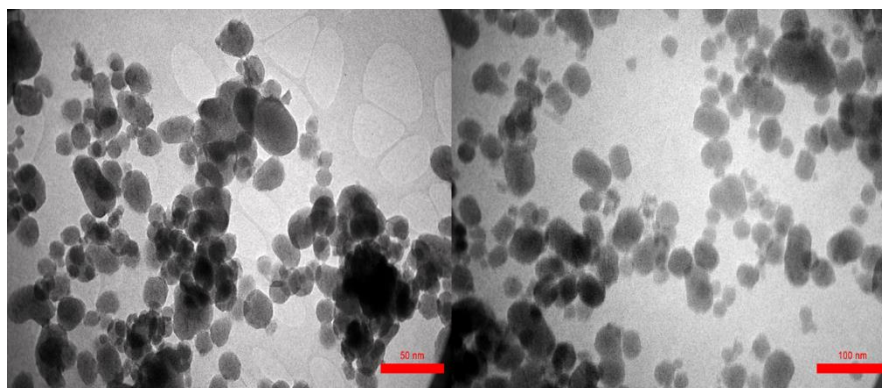


Figure 7. TEM image of MCM-41 catalyst

indicates the optimal conditions. The orthogonal arrays are represented by the following formula: $L_n(X^y)$, where n is the value of the designed experiments, where X is the number of levels, and y is the maximum value of the factors [66]. After introducing the studied factors and related to the levels, the results of the S/N ratio, nine experiments were obtained by Taguchi software which is shown in (Table 4). According to Figure 8, the highest removal conditions of BTEXS cyclic hydrocarbons were obtained at pH = 11; time 60 minutes, the concentration of 100 mg/kg, and a dose of 0.5 g of MCM-41 catalyst. According to Figure 9, an evaluation of the obtained data showed that pH has the most minor importance and interaction in the removal efficiency of BTEXS. According to the graphs obtained from the Taguchi experiment, it was found that the highest removal of BTEXS cyclic hydrocarbons in an aqueous solution is related to experiment number four, in which the results of GC, COD, and TOC also indicate and confirm each other.

- Relation of COD and TOC to an aqueous, solution containing BTEXS cyclic hydrocarbons

Due to the similarity of the COD to TOC ratio from the results of nine experiments, and previous research [67]. The COD and TOC results of this study were related, and the approximate formula for the two was obtained, which can be considered in future research. According to Figure 10, the results showed that if the value obtained from the

TOC test is multiplied by 4.2, the numerical value of COD is obtained.

- Removal of cyclic hydrocarbons using MCM-41 catalyst in the presence of H₂O₂

At this stage of the experiment, the highest and lowest removal points of BTEXS cyclic hydrocarbons in an aqueous solution were investigated. According to Taguchi's results, Experiment 3 had the lowest removal

Table 4. Responses, S/N ratio, and removal

Taguchi RUN	GC (%)	COD (%)	TOC (%)	S/N Ratio
1	26.21	24.66	24.81	28.027
2	16.72	16.22	16.5	24.336
3	15.3	14.83	15.14	23.571
4	70.12	70.12	70.06	36.914
5	49.43	50	50.12	33.952
6	41.8	40.07	40	32.17
7	37.01	37.04	37.05	31.371
8	31.76	32.63	32.51	30.182
9	30.2	30.32	30.32	30.016

Remark: The Taguchi run (Efficiency%) is the total BTEXS. Average signal-to-noise (average of 18 samples made) output from Taguchi software.

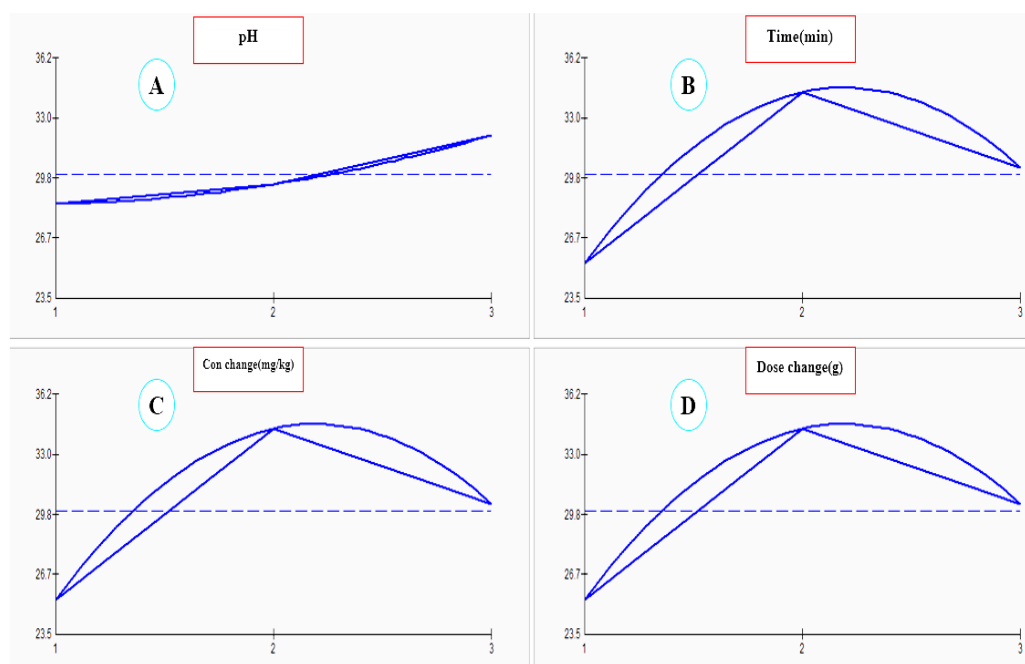


Figure 8. Effect of parameters on the removal of cyclic hydrocarbons under optimal conditions: A) pH, B) Time (minutes), C) Concentration change (mg/kg), and D) MCM-41 catalyst dose (g)

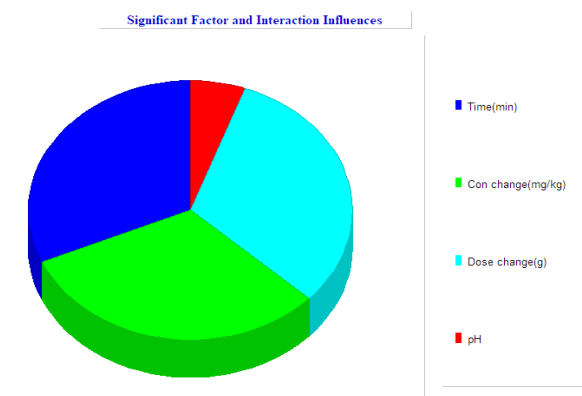


Figure 9. Interaction and significant factors in the optimal conditions were obtained from Taguchi software

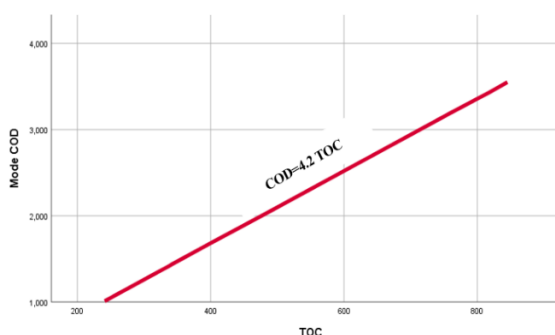
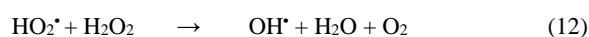


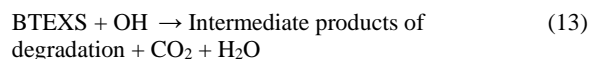
Figure 10. COD and TOC relationship diagram for an aqueous solution containing BTEXS cyclic hydrocarbons

efficiency, and Experiment 4 had the highest removal efficiency. Experimental steps were performed in the presence of hydrogen peroxide in these two experiments. The amount of hydrogen peroxide used in the first experiment was 183 mg/kg, which means that approximately 6% of the hydrogen peroxide in this aqueous solution containing cyclic hydrocarbons was used. In an acidic environment, according to the results

obtained from GC, the reaction was not performed well at the desired time; the amount of hydrogen peroxide used in the second experiment was calculated to be 538.5 mg/kg, which means that approximately 19% of the hydrogen peroxide in this aqueous solution containing cyclic hydrocarbons was used. In other words, in an alkaline environment, the reaction is done well at the desired time. Hydrogen peroxide may act as an additional source of hydroxyl radicals and enhance the degradation process resulting from the removal of organic pollutants (Equations (7)-(13)) [68] The results of this study showed that by increasing the concentration of hydrogen peroxide, the efficiency of removing pollutants increases and it has been confirmed by other similar studies [69-71].



In fact the hydroxyl free radical generated from hydrogen peroxide can degrade BTEXS to simple intermediate products as stated below [72]:



The result of the results (Figure 11) is that in two experiments, the removal of cyclic hydrocarbons BTEXS in the presence of hydrogen peroxide increased in the presence of alkaline pH and increased in the absence of 4%. Hydrogen peroxide did not show a significant change in acidic pH. The results also confirm with data reported in literature [3] at alkaline conditions.

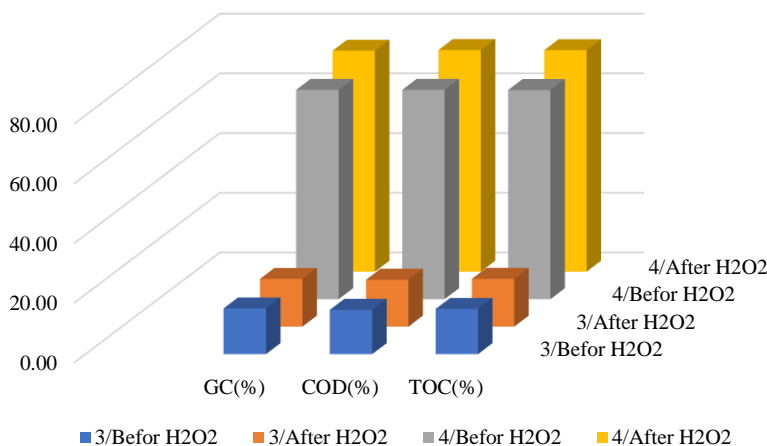


Figure 11. A comparison of GC, COD, and TOC results before and after hydrogen peroxide addition

Removal of cyclic hydrocarbons using MCM-41 catalyst on actual industrial effluent sample

For this research stage, an actual sample of industrial effluent containing cyclic hydrocarbons was selected. The average of last year's data of cyclic hydrocarbons of industrial effluent samples showed that its value is close to level 2 of the standard sample test. Due to the changing conditions of the industrial wastewater, the reason for choosing three different concentrations for Taguchi software was to be able to examine the removal of contaminants to a greater or lesser extent by the MCM-41 catalyst. The final data are given in Table 5. According to Figure 12, one of the reasons for the 3% increase in the removal, of industrial wastewater samples could be less material in the structure of industrial wastewater, which has led to a 4.52 % increase compared to the previous sample in the standard state. The amount of xylene in industrial wastewater samples is close to zero. The numbers obtained are confirmed by the results and previous coverage. Accordingly, MCM-41 Catalyst is a promising approach for the treatment of wastewater containing organic pollutants like BTEXS.

Table 5. General data of optimal standard sample and industrial wastewater sample

No.	Sample Name	COD (%)	TOC (%)	GC (%)
1	Standard optimized sample+H2O2	74.26	74.22	74.02
2	Standard optimized sample	70.12	70.06	70.12
3	Sample of industrial wastewater+H2O2	77.36	77.33	76.8
4	Sample of industrial wastewater	72.84	72.79	72.62

Remark: Final comparison of the removal percentage of cyclic hydrocarbons in the optimal standard solution and the sample of industrial wastewater

MCM-41 catalyst reusability

As seen from the scan of (Figure 13), at each step of the wash, the amount of hydrocarbon output in methanol showed a decreasing trend, indicating that it was completely removed from the MCM-41 catalyst.

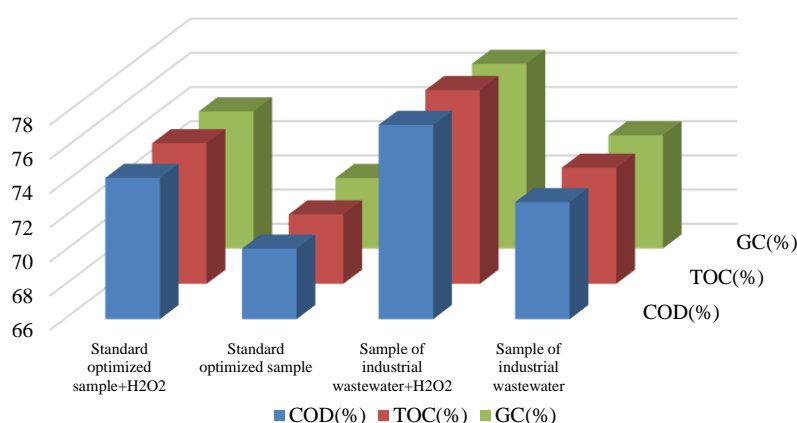


Figure 12. General comparison chart of optimal standard sample and industrial wastewater sample

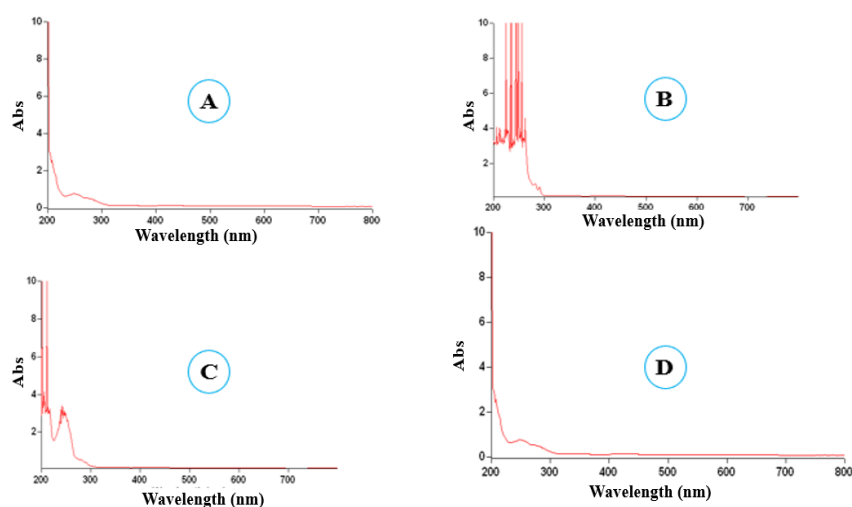


Figure 13. Absorption at a wavelength of 200 to 800 nm, A) pure methanol, B) first washing, B) second washing, and C) third washing

The reduced catalyst was re-weighed on a digital scale, and its final weight after reduction was 0.5001 g. The conclusion that can be drawn from the weight of the catalyst before and after reduction is that we did not have the amount of MCM-41 catalyst during the weight loss process, and the catalyst can be reused after reduction. The bias values of the initial and final weight of the catalyst are less than 5%. The results showed that the reduced MCM-41 catalyst can be reused.

• Regeneration of MCM-41

As shown in (Figure 14), after eight of reconstitution periods, the removal efficiency of MCM-41 to BTEXS in an aqueous solution remains above 90%, indicating that MCM-41 has a good performance after reconstitution. MCM-41 remains a mesoporous structure and has the potential to regenerate after the reaction. The results of our group also confirmed the results of the research [57]. Future work could focus on further improving the MCM-41 regeneration performance with other solvents.

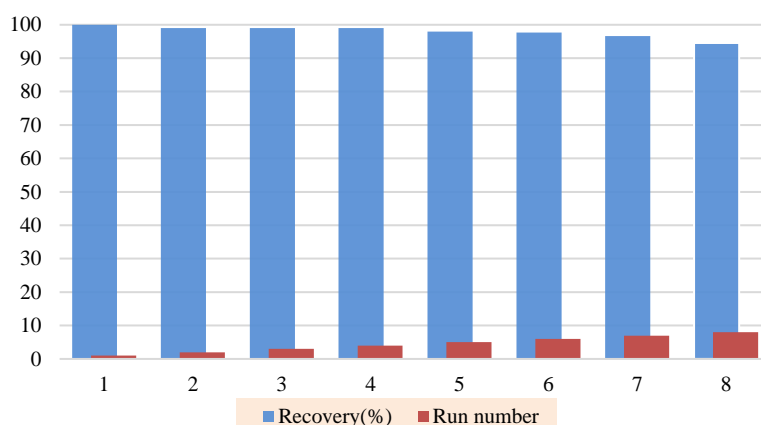


Figure 14. BTEXS removal recovery by MCM-41 catalyst after repeated reconstructions

CONCLUSIONS

The present work investigates the performance of a catalyst (MCM-41) in the adsorption of BTEXS cyclic hydrocarbons at 24 °C. The results showed that the catalyst with a dose of 0.5 g, a reaction time of 60 minutes, the number of cyclic hydrocarbons of 100 mg/l, and pH=11 of major catalytic activities. In addition, COD analysis and analysis show that in addition to the removal of cyclic hydrocarbons, by reducing cyclic hydrocarbons, the systems can reduce the average mineralization of organic matter in solution. The three parameters of catalyst dose, cyclic hydrocarbon concentration, and reaction time; had the largest share in MCM-41 catalyst activity, according to Taguchi's results. In catalyst reusability tests, the highest catalytic activity was present in the reaction cycles of eight consecutive cycles.

FUNDING

This research did not receive any specific grant from funding agencies in the public, commercial, or not-for-profit sectors.

CREDIT AUTHORSHIP CONTRIBUTION STATEMENT

Mohammad Heydari: Conceptualization, Data curation, Writing - original draft, Resources, Software, Data curation.

Tayebeh Tabatabaie: Validation, review & editing, Supervision, Data curation. **Fazel Amiri:** Validation, review & editing, Supervision, Data curation.

Seyed Enayat Hashemi: Validation, review & editing, Supervision, Data curation.

DECLARATION OF COMPETING INTEREST

This research did not receive any specific grant from funding agencies in the public, commercial, or not-for-profit sectors.

DATA AVAILABILITY

The datasets generated during and, or analyzed during the current study are available from the corresponding authors on reasonable request.

ACKNOWLEDGMENTS

This research has been extracted from a Ph.D. thesis at Islamic Azad University, Bushehr. The authors would like to acknowledge the Pars laboratory for providing facilities and equipment as well as my dear colleagues for their countless cooperation and e during this research.

REFERENCES

- Vandana, M. Priyadarshane, U. Mahto and S. Das, 2022. Chapter 2 - Mechanism of Toxicity and Adverse Health Effects of Environmental Pollutants, in *Microbial Biodegradation and Bioremediation (Second Edition)*, S. Das and H.R. Dash, Editors., Elsevier. p. 33-53. Doi: <https://doi.org/10.1016/B978-0-323-85455-9.00024-2>
- Murungi, P.I. and A.A. Sulaimon, 2022. Petroleum Sludge Treatment and Disposal Techniques: A Review. *Environmental Science and Pollution Research*. Doi: 10.1007/s11356-022-19614-z
- Farias, M.F., Y.S. Domingos, G.J. Turolla Fernandes, F.L. Castro, V.J. Fernandes, M.J. Fonseca Costa and A.S. Araujo, 2018. Effect of Acidity in the Removal-Degradation of Benzene in Water Catalyzed by Co-Mcm-41 in Medium Containing Hydrogen Peroxide. *Microporous and Mesoporous Materials*, 258, pp: 33-40. Doi: <https://doi.org/10.1016/j.micromeso.2017.09.003>
- Ziabari, S.E.H., T. Tabatabaie, F. Amiri and B. Ramavandi, 2022. Spatial Distribution of Btx Emission and Health Risk Assessment in the Ambient Air of Pars Special Economic Energy Zone (Pseez) Using Passive Sampling. *Environmental Monitoring and Assessment*, 194(2), pp: 1-18. Doi: <https://doi.org/10.1007/s10661-022-09767-2>
- Wongbunmak, A., Y. Panthongkham, M. Suphantharika and T. Pongtharangkul, 2021. A Fixed-Film Bioscrubber of Microbacterium Esteraromaticum Sbs1-7 for Toluene/Styrene Biodegradation. *Journal of Hazardous Materials*, 418pp: 126287. Doi: <https://doi.org/10.1016/j.jhazmat.2021.126287>
- Halder, S., Z. Xie, M.H. Nantz and X.-A. Fu, 2022. Integration of a Micropreconcentrator with Solid-Phase Microextraction for Analysis of Trace Volatile Organic Compounds by Gas Chromatography-Mass Spectrometry. *Journal of Chromatography A*, 1673, pp: 463083. Doi: <https://doi.org/10.1016/j.chroma.2022.463083>
- Wu, X., Q. Hou, J. Huang, J. Chai and F. Zhang, 2021. Exploring the Oh-Initiated Reactions of Styrene in the Atmosphere and the Role of Van Der Waals Complex. *Chemosphere*, 282, pp: 131004. Doi: <https://doi.org/10.1016/j.chemosphere.2021.131004>
- Moshiran, V.A., A. Karimi, F. Golbabaei, M.S. Yarandi, A.A. Sajedian and A.G. Koozekonan, 2021. Quantitative and Semiquantitative Health Risk Assessment of Occupational Exposure to Styrene in a Petrochemical Industry. *Safety and Health at Work*, 12(3), pp: 396-402. Doi: <https://doi.org/10.1016/j.shaw.2021.01.009>
- Yu, B., Z. Yuan, Z. Yu and F. Xue-song, 2022. Btx in the Environment: An Update on Sources, Fate, Distribution, Pretreatment, Analysis, and Removal Techniques. *Chemical Engineering Journal*, 435, pp: 134825. Doi: <https://doi.org/10.1016/j.cej.2022.134825>
- Li, K., Y. He, J. Li, J. Sheng, Y. Sun, J. Li and F. Dong, 2021. Identification of Deactivation-Resistant Origin of in(OH)3 for Efficient and Durable Photodegradation of Benzene, Toluene and Their Mixtures. *Journal of Hazardous Materials*, 416, pp: 126208. Doi: <https://doi.org/10.1016/j.jhazmat.2021.126208>
- Muneron Mello, J.M., H.L. Brandão, A. Valério, A.A.U. de Souza, D. de Oliveira, A. da Silva and S.M.A.G.U. de Souza, 2019. Biodegradation of Btx Compounds from Petrochemical Wastewater: Kinetic and Toxicity. *Journal of Water Process Engineering*, 32, pp: 100914. Doi: <https://doi.org/10.1016/j.jwpe.2019.100914>
- Tang, W., X. Li, H. Liu, S. Wu, Q. Zhou, C. Du, Q. Teng, Y. Zhong and C. Yang, 2020. Sequential Vertical Flow Trickling Filter and Horizontal Flow Multi-Soil-Layering Reactor for Treatment of Decentralized Domestic Wastewater with Sodium Dodecyl Benzene Sulfonate. *Bioresour Technol*, 300, pp: 122634. Doi: <https://doi.org/10.1016/j.biortech.2019.122634>
- Ma, Z., D. Yao, J. Zhao, H. Li, Z. Chen, P. Cui, Z. Zhu, L. Wang, Y. Wang, Y. Ma and J. Gao, 2021. Efficient Recovery of Benzene and N-Propanol from Wastewater Via Vapor Recompression Assisted Extractive Distillation Based on Techno-Economic and Environmental Analysis. *Process Safety and Environmental Protection*, 148, pp: 462-472. Doi: <https://doi.org/10.1016/j.psep.2020.10.033>
- Casado, E., M.C. Garcia, D.A. Krawczyk, F.J. Romero-Salguero and A. Rodero, 2020. Study of the Plasma-Liquid Interaction for an Argon Nonthermal Microwave Plasma Jet from the Analysis of Benzene Degradation. *Plasma Processes and Polymers*, 17(9), pp: 2000030. Doi: <https://doi.org/10.1002/ppap.202000030>
- Piekutin, J., 2021. The Identification of Fouling in Reverse Osmosis in Reverse Osmosis in the Treatment of Water with Petroleum Substances. *Water*, 13(8), pp: 1092. Doi: <https://doi.org/10.3390/w13081092>
- Guo, Y., Q. Xue, H. Zhang, N. Wang, S. Chang, Y. Fang, H. Wang, F. Yuan, H. Pang and H. Chen, 2018. Highly Efficient Treatment of Real Benzene Dye Intermediate Wastewater by Simple Limestone and Lime Neutralization-Coagulation with Improved Fenton Oxidation. *Environmental Science and Pollution Research*, 25(31), pp: 31125-31135. Doi: 10.1007/s11356-018-3101-0
- da Costa, J.S., E.G. Bertizzolo, D. Bianchini and A.R. Fajardo, 2021. Adsorption of Benzene and Toluene from Aqueous Solution Using a Composite Hydrogel of Alginate-Grafted with Mesoporous Silica. *Journal of Hazardous Materials*, 418, pp: 126405. Doi: <https://doi.org/10.1016/j.jhazmat.2021.126405>
- Gu, W., J. Guo, J. Bai, B. Dong, J. Hu, X. Zhuang, C. Zhang and K. Shih, 2022. Co-Pyrolysis of Sewage Sludge and Ca(H2PO4)2: Heavy Metal Stabilization, Mechanism, and Toxic Leaching. *Journal of Environmental Management*, 305, pp: 114292. Doi: <https://doi.org/10.1016/j.jenvman.2021.114292>
- Abdullah, F.H., N.H.H.A. Bakar and M.A. Bakar, 2022. Current Advancements on the Fabrication, Modification, and Industrial Application of Zinc Oxide as Photocatalyst in the Removal of Organic and Inorganic Contaminants in Aquatic Systems. *Journal of Hazardous Materials*, 424, pp: 127416. Doi: <https://doi.org/10.1016/j.jhazmat.2021.127416>
- Crini, G., C. Cosentino, C. Bradu, M. Fourmentin, G. Torri, O. Ruzimuradov, I.A. Alaton, M.C. Tomei, J. Derco, M. Barhoumi, H. Prosen, B.N. Malinović, M. Vrabel, M.M. Huq, J. Soltan, E. Lichtfouse and N. Morin-Crini, 2022. Innovative Technologies to Remove Alkylphenols from Wastewater: A Review. *Environmental Chemistry Letters*. Doi: 10.1007/s10311-022-01438-5
- Madhubashani, A.M.P., D.A. Giannakoudakis, B.M.W.P.K. Amarasinghe, A.U. Rajapaksha, P.B.T. Pradeep Kumara, K.S. Triantafyllidis and M. Vithanage, 2021. Propensity and Appraisal of Biochar Performance in Removal of Oil Spills: A Comprehensive Review. *Environmental Pollution*, 288, pp: 117676. Doi: <https://doi.org/10.1016/j.envpol.2021.117676>
- Mohammad, Y., E. Shaibu-Imodagbe, S. Igboro, A. Giwa and C. Okuofu, 2014. Adsorption of Phenol from Refinery Wastewater Using Rice Husk Activated Carbon. *Iranian (Iranica) Journal of*

- Energy & Environment*, 5(4), pp 393-399. Doi: 10.5829/idosi.ijee.2014.05.04.07
23. Costa, J.A.S., R.A. de Jesus, D.O. Santos, J.B. Neris, R.T. Figueiredo and C.M. Paranhos, 2021. Synthesis, Functionalization, and Environmental Application of Silica-Based Mesoporous Materials of the M41s and Sba-N Families: A Review. *Journal of Environmental Chemical Engineering*, 9(3), pp: 105259. Doi: <https://doi.org/10.1016/j.jece.2021.105259>
 24. Costa, J.A.S., R.A. de Jesus, D.O. Santos, J.F. Mano, L.P.C. Romão and C.M. Paranhos, 2020. Recent Progresses in the Adsorption of Organic, Inorganic, and Gas Compounds by Mcm-41-Based Mesoporous Materials. *Microporous and Mesoporous Materials*, 291, pp: 109698. Doi: <https://doi.org/10.1016/j.micromeso.2019.109698>
 25. Jankowska, A., A. Chłopek, A. Kowalczyk, M. Rutkowska, W. Mozgawa, M. Michalik, S. Liu and L. Chmielarz, 2021. Enhanced Catalytic Performance in Low-Temperature NH₃-SCR Process of Spherical Mcm-41 Modified with Cu by Template Ion-Exchange and Ammonia Treatment. *Microporous and Mesoporous Materials*, 315, pp: 110920. Doi: <https://doi.org/10.1016/j.micromeso.2021.110920>
 26. Bahari, M.B., A.A. Jalil, C.R. Mamat, N.S. Hassan, H.D. Setiabudi and D.V.N. Vo, 2022. Insight into the Development of Silica-Based Materials as Photocatalysts for CO₂ Photoconversion Towards CH₃OH: A Review and Recent Progress. *Surfaces and Interfaces*, 31, pp: 102049. Doi: <https://doi.org/10.1016/j.surfin.2022.102049>
 27. Habeche, F., M. Hachemaoui, A. Mokhtar, K. Chikh, F. Benali, A. Mekki, F. Zaoui, Z. Cherifi and B. Boukoussa, 2020. Recent Advances on the Preparation and Catalytic Applications of Metal Complexes Supported-Mesoporous Silica Mcm-41 (Review). *Journal of Inorganic and Organometallic Polymers and Materials*, 30(11), pp: 4245-4268. Doi: 10.1007/s10904-020-01689-1
 28. Kwan, W.H. and Y.S. Wong, 2020. Acid Leached Rice Husk Ash (Arha) in Concrete: A Review. *Materials Science for Energy Technologies*, 3, pp: 501-507. Doi: <https://doi.org/10.1016/j.mset.2020.05.001>
 29. AbuKhadra, M.R., A.S. Mohamed, A.M. El-Sherbeeney and M.A. Elmeligy, 2020. Enhanced Photocatalytic Degradation of Acephate Pesticide over Mcm-41/Co₃O₄ Nanocomposite Synthesized from Rice Husk Silica Gel and Peach Leaves. *Journal of Hazardous Materials*, 389, pp: 122129. Doi: <https://doi.org/10.1016/j.jhazmat.2020.122129>
 30. Cheng, Z., J. Li, P. Yang and S. Zuo, 2018. Preparation of Mnco/Mcm-41 Catalysts with High Performance for Chlorobenzene Combustion. *Chinese Journal of Catalysis*, 39(4), pp: 849-856. Doi: [https://doi.org/10.1016/S1872-2067\(17\)62950-4](https://doi.org/10.1016/S1872-2067(17)62950-4)
 31. Liou, T.-H. and P.-Y. Wang, 2020. Utilization of Rice Husk Wastes in Synthesis of Graphene Oxide-Based Carbonaceous Nanocomposites. *Waste Management*, 108pp: 51-61. Doi: <https://doi.org/10.1016/j.wasman.2020.04.029>
 32. Kanthe, V., 2021. Effect of Superplasticizer on Strength and Durability of Rice Husk Ash Concrete. *Iranian (Iranica) Journal of Energy & Environment*, 12(3), pp: 204-208. Doi: 10.5829/ijee.2021.12.03.04
 33. Odeyemi, S., R. Abdulwahab, M. Akinpelu, R. Afolabi and O. Atoyebi, 2022. Strength Properties of Steel and Bamboo Reinforced Concrete Containing Quarry Dust, Rice Husk Ash and Guinea Corn Husk Ash. *Iranian (Iranica) Journal of Energy & Environment*, 13(4), pp: 354-362. Doi: 10.5829/ijee.2022.13.04.05
 34. Liu, Y., C. Li, A. Peyravi, Z. Sun, G. Zhang, K. Rahmani, S. Zheng and Z. Hashisho, 2021. Mesoporous Mcm-41 Derived from Natural Opoka and Its Application for Organic Vapors Removal. *Journal of Hazardous Materials*, 408, pp: 124911. Doi: <https://doi.org/10.1016/j.jhazmat.2020.124911>
 35. Liu, Y., J. Liao, L. Chang and W. Bao, 2022. Ag Modification of Sba-15 and Mcm-41 Mesoporous Materials as Sorbents of Thiophene. *Fuel*, 311, pp: 122537. Doi: <https://doi.org/10.1016/j.fuel.2021.122537>
 36. Ye, Z., J.M. Giraudon, N. Nuns, P. Simon, N. De Geyter, R. Morent and J.F. Lamonier, 2018. Influence of the Preparation Method on the Activity of Copper-Manganese Oxides for Toluene Total Oxidation. *Applied Catalysis B: Environmental*, 223, pp: 154-166. Doi: <https://doi.org/10.1016/j.apcatb.2017.06.072>
 37. Dong, Y., J. Sun, X. Ma, W. Wang, Z. Song, X. Zhao, Y. Mao and W. Li, 2022. Study on the Synergy Effect of MnO_x and Support on Catalytic Ozonation of Toluene. *Chemosphere*, 303, pp: 134991. Doi: <https://doi.org/10.1016/j.chemosphere.2022.134991>
 38. Ma, M., K. Gao, D. Zhao, X. Ma and Z. Ma, 2022. Effect of Process Conditions on Reaction-Type Adsorption of O-Xylene by Mcm-41 Supported Sulfuric Acid: Model Simulations of Breakthrough Curves. *Journal of Environmental Chemical Engineering*, 10(1), pp: 106937. Doi: <https://doi.org/10.1016/j.jece.2021.106937>
 39. Li, X., J. Wang, Y. Guo, T. Zhu and W. Xu, 2021. Adsorption and Desorption Characteristics of Hydrophobic Hierarchical Zeolites for the Removal of Volatile Organic Compounds. *Chemical Engineering Journal*, 411, pp: 128558. Doi: <https://doi.org/10.1016/j.cej.2021.128558>
 40. Andas, J., S.H. Ekhbal and T.H. Ali, 2021. Mcm-41 Modified Heterogeneous Catalysts from Rice Husk for Selective Oxidation of Styrene into Benzaldehyde. *Environmental Technology & Innovation*, 21, pp: 101308. Doi: <https://doi.org/10.1016/j.eti.2020.101308>
 41. Gao, K., M. Ma, Y. Liu and Z. Ma, 2021. A Comparative Study of the Removal of O-Xylene from Gas Streams Using Mesoporous Silicas and Their Silica Supported Sulfuric Acids. *Journal of Hazardous Materials*, 409, pp: 124965. Doi: <https://doi.org/10.1016/j.jhazmat.2020.124965>
 42. Li, Y., N. Bonyadi and B. Lee, 2022. A Parallel Decomposition Approach for Building Design Optimization. *Journal of Building Engineering*, 54, pp: 104574. Doi: <https://doi.org/10.1016/j.jobe.2022.104574>
 43. Zhang, F., M. Wang and M. Yang, 2021. Successful Application of the Taguchi Method to Simulated Soil Erosion Experiments at the Slope Scale under Various Conditions. *CATENA*, 196, pp: 104835. Doi: <https://doi.org/10.1016/j.catena.2020.104835>
 44. Kechagias, J.D., K.-E. Aslani, N.A. Fountas, N.M. Vaxevanidis and D.E. Manolagos, 2020. A Comparative Investigation of Taguchi and Full Factorial Design for Machinability Prediction in Turning of a Titanium Alloy. *Measurement*, 151, pp: 107213. Doi: <https://doi.org/10.1016/j.measurement.2019.107213>
 45. Dagdevir, T. and V. Ozceyhan, 2021. Optimization of Process Parameters in Terms of Stabilization and Thermal Conductivity on Water Based TiO₂ Nanofluid Preparation by Using Taguchi Method and Grey Relation Analysis. *International Communications in Heat and Mass Transfer*, 120, pp: 105047. Doi: <https://doi.org/10.1016/j.icheatmasstransfer.2020.105047>
 46. Ikeagwuani, C.C., D.C. Nwonu, C.K. Ugwu and C.C. Agu, 2020. Process Parameters Optimization for Eco-Friendly High Strength Sandcrete Block Using Taguchi Method. *Heliyon*, 6(6), pp: e04276. Doi: <https://doi.org/10.1016/j.heliyon.2020.e04276>
 47. Schleinkofer, U., M. Dazer, K. Lucan, O. Mannuß, B. Bertsche and T. Bauernhansl, 2019. Framework for Robust Design and Reliability Methods to Develop Frugal Manufacturing Systems. *Procedia CIRP*, 81, pp: 518-523. Doi: <https://doi.org/10.1016/j.procir.2019.03.148>

48. Madu, I.E. and C.N. Madu, 1999. Design Optimization Using Signal-to-Noise Ratio. *Simulation Practice and Theory*, 7(4), pp: 349-372. Doi: [https://doi.org/10.1016/S0928-4869\(99\)00008-7](https://doi.org/10.1016/S0928-4869(99)00008-7)
49. Sathish Kumar, T., R. Vignesh, B. Ashok, P. Saiteja, A. Jacob, C. Karthick, A.K. Jeevanantham, M. Senthilkumar and K. Muhammad Usman, 2022. Application of Statistical Approaches in Ic Engine Calibration to Enhance the Performance and Emission Characteristics: A Methodological Review. *Fuel*, 324, pp: 124607. Doi: <https://doi.org/10.1016/j.fuel.2022.124607>
50. Nayak, P. and A. Datta, 2021. Synthesis of Sio₂-Nanoparticles from Rice Husk Ash and Its Comparison with Commercial Amorphous Silica through Material Characterization. *Silicon*, 13(4), pp: 1209-1214. Doi: <https://doi.org/10.1007/s12633-020-00509-y>
51. Kamari, S. and F. Ghorbani, 2021. Extraction of Highly Pure Silica from Rice Husk as an Agricultural by-Product and Its Application in the Production of Magnetic Mesoporous Silica Mcm-41. *Biomass Conversion and Biorefinery*, 11(6), pp: 3001-3009. Doi: <https://doi.org/10.1007/s13399-020-00637-w>
52. Cai, Q., Z.-S. Luo, W.-Q. Pang, Y.-W. Fan, X.-H. Chen and F.-Z. Cui, 2001. Dilute Solution Routes to Various Controllable Morphologies of Mcm-41 Silica with a Basic Medium. *Chemistry of materials*, 13(2), pp: 258-263. Doi: <https://doi.org/10.1021/cm990661z>
53. Amanollahi, H., G. Moussavi and S. Giannakis, 2019. Vuv/Fe(II)/H₂O₂ as a Novel Integrated Process for Advanced Oxidation of Methyl Tert-Butyl Ether (Mtbe) in Water at Neutral Ph: Process Intensification and Mechanistic Aspects. *Water Research*, 166, pp: 115061. Doi: <https://doi.org/10.1016/j.watres.2019.115061>
54. Zhong, J., J. Huang, Y. Liu, D. Li, C. Tan, P. Chen, H. Liu, X. Zheng, C. Wen, W. Lv and G. Liu, 2022. Construction of Double-Functionalized G-C₃N₄ Heterojunction Structure Via Optimized Charge Transfer for the Synergistically Enhanced Photocatalytic Degradation of Sulfonamides and H₂O₂ Production. *Journal of Hazardous Materials*, 422, pp: 126868. Doi: <https://doi.org/10.1016/j.jhazmat.2021.126868>
55. Cai, H., X. Liu, J. Zou, J. Xiao, B. Yuan, F. Li and Q. Cheng, 2018. Multi-Wavelength Spectrophotometric Determination of Hydrogen Peroxide in Water with Peroxidase-Catalyzed Oxidation of Abts. *Chemosphere*, 193, pp: 833-839. Doi: <https://doi.org/10.1016/j.chemosphere.2017.11.091>
56. Klaewkla, R., T. Rirkomboon, S. Kulprathipanja, L. Nemeth and P. Rangsunvigit, 2006. Light Sensitivity of Phenol Hydroxylation with Ts-1. *Catalysis Communications*, 7(5), pp: 260-263. Doi: <https://doi.org/10.1016/j.catcom.2005.10.015>
57. Sharma, S., U.P. Singh and A.P. Singh, 2021. Synthesis of Mcm-41 Supported Cobalt (II) Complex for the Formation of Polyhydroquinoline Derivatives. *Polyhedron*, 199, pp: 115102. Doi: <https://doi.org/10.1016/j.poly.2021.115102>
58. Ullah, Z., Z. Man, A.S. Khan, N. Muhammad, H. Mahmood, O. Ben Ghanem, P. Ahmad, M.-U. Hassan Shah, R. Mamoon Ur and M. Raheel, 2019. Extraction of Valuable Chemicals from Sustainable Rice Husk Waste Using Ultrasonic Assisted Ionic Liquids Technology. *Journal of Cleaner Production*, 220, pp: 620-629. Doi: <https://doi.org/10.1016/j.jclepro.2019.02.041>
59. Santana Costa, J.A. and C.M. Paranhos, 2018. Systematic Evaluation of Amorphous Silica Production from Rice Husk Ashes. *Journal of Cleaner Production*, 192, pp: 688-697. Doi: <https://doi.org/10.1016/j.jclepro.2018.05.028>
60. Saloni, Parveen and T.M. Pham, 2020. Enhanced Properties of High-Silica Rice Husk Ash-Based Geopolymer Paste by Incorporating Basalt Fibers. *Construction and Building Materials*, 245, pp: 118422. Doi: <https://doi.org/10.1016/j.conbuildmat.2020.118422>
61. Gao, Y., R.-y. Zhou, L. Yao, W. Yin, J.-x. Yu, Q. Yue, Z. Xue, H. He and B. Gao, 2022. Synthesis of Rice Husk-Based Ion-Imprinted Polymer for Selective Capturing Cu(II) from Aqueous Solution and Re-Use of Its Waste Material in Glaser Coupling Reaction. *Journal of Hazardous Materials*, 424, pp: 127203. Doi: <https://doi.org/10.1016/j.jhazmat.2021.127203>
62. Robotjazi, Z.S., M.R. Naimi-Jamal and M. Tajbakhsh, 2022. Synthesis and Characterization of Highly Efficient and Recoverable Cu@Mcm-41-(2-Hydroxy-3-Propoxypropyl) Metformin Mesoporous Catalyst and Its Uses in Ullmann Type Reactions. *Scientific Reports*, 12(1), pp: 4949. Doi: 10.1038/s41598-022-08902-w
63. Viswanadham, B., V. Vishwanathan, K.V.R. Chary and Y. Satyanarayana, 2021. Catalytic Dehydration of Glycerol to Acrolein over Mesoporous Mcm-41 Supported Heteropolyacid Catalysts. *Journal of Porous Materials*, 28(4), pp: 1269-1279. Doi: 10.1007/s10934-021-01070-8
64. A. Mannaa, M., H.M. Altass and R.S. Salama, 2021. Mcm-41 Grafted with Citric Acid: The Role of Carboxylic Groups in Enhancing the Synthesis of Xanthenes and Removal of Heavy Metal Ions. *Environmental Nanotechnology, Monitoring & Management*, 15, pp: 100410. Doi: <https://doi.org/10.1016/j.enmm.2020.100410>
65. Mehdinia, S.M., K. Moeinian and T. Rastgoo, 2014. Rice Husk Silica Adsorbent for Removal of Hexavalent Chromium Pollution from Aquatic Solutions. *Iranica Journal of Energy & Environment*, 5(2), pp: 218-223. Doi: 10.5829/idosi.ijee.2014.05.02.15
66. Narges Elmi, F. and F. Reza, 2018. Optimization of Operating Parameters in Photocatalytic Activity of Visible Light Active Ag/Tio₂ Nanoparticles. *Russian Journal of Physical Chemistry A*, 92(13), pp: 2835-2846. Doi: 10.1134/S0036024418130071
67. Hua, X., X. Song, M. Yuan and D. Donga, 2011. The Factors Affecting Relationship between Cod and Toc of Typical Papermaking Wastewater, in Advances in Computer Science, Intelligent System and Environment. Springer. p. 239-244. Doi: https://doi.org/10.1007/978-3-642-23756-0_39
68. Liu, Y., Y. Zhao and J. Wang, 2021. Fenton/Fenton-Like Processes with in-Situ Production of Hydrogen Peroxide/Hydroxyl Radical for Degradation of Emerging Contaminants: Advances and Prospects. *Journal of Hazardous Materials*, 404, pp: 124191. Doi: <https://doi.org/10.1016/j.jhazmat.2020.124191>
69. Suh, J.H. and M. Mohseni, 2004. A Study on the Relationship between Biodegradability Enhancement and Oxidation of 1,4-Dioxane Using Ozone and Hydrogen Peroxide. *Water Research*, 38(10), pp: 2596-2604. Doi: <https://doi.org/10.1016/j.watres.2004.03.002>
70. Farhadi, N., T. Tabatabaie, B. Ramavandi and F. Amiri, 2021. Ibufrofen Elimination from Water and Wastewater Using Sonication/Ultraviolet/Hydrogen Peroxide/Zeolite-Titanate Photocatalyst System. *Environmental Research*, 198, pp: 111260. Doi: <https://doi.org/10.1016/j.envres.2021.111260>
71. Bellouk, H., I.E. Mrabet, K. Tanji, M. Nawdali, M. Benzina, M. Eloussaief and H. Zaitan, 2022. Performance of Coagulation-Flocculation Followed by Ultra-Violet/Ultrasound Activated Persulfate/Hydrogen Peroxide for Landfill Leachate Treatment. *Scientific African*, 17, pp: e01312. Doi: <https://doi.org/10.1016/j.sciaf.2022.e01312>
72. Chen, Z., M. Fu, C. Yuan, X. Hu, J. Bai, R. Pan, P. Lu and M. Tang, 2022. Study on the Degradation of Tetracycline in Wastewater by Micro-Nano Bubbles Activated Hydrogen Peroxide. *Environmental Technology*, 43(23), pp: 3580-3590. Doi: 10.1080/09593330.2021.1928292

COPYRIGHTS

©2023 The author(s). This is an open access article distributed under the terms of the Creative Commons Attribution (CC BY 4.0), which permits unrestricted use, distribution, and reproduction in any medium, as long as the original authors and source are cited. No permission is required from the authors or the publishers.



Persian Abstract

چکیده

حجم زیادی از فاضلاب صنعتی آلوده باعث نگرانی فزاینده‌ای در بین محققان و دستداران محیط زیست شده است. هیدروکربن‌های حلقوی بنزن، تولوئن، اتیل بنزن، زایلن و استایرن (BTEXS) در پساب‌های صنعتی اغلب در برابر تجزیه بیولوژیکی کاملاً پایدار هستند و باید قبل از دفع، تصفیه شوند. در این زمینه، استفاده از فرآیندهای جذب یک جایگزین بالقوه برای تصفیه طیف وسیعی از آلاینده‌های آلی، به‌ویژه ترکیبات معطر در پساب‌های صنعتی است. این مطالعه به بررسی تهیه MCM-41 از سیلیس پرداخته است. ماده استخراج شده از خاکستر پوسته برنج MCM-41 سبز سنتز شد تا اثر مزوپور مورد استفاده در حذف BTEXS از یک محیط آبی با استفاده از روش تاگوچی ارزیابی شود. محلول آبی حاوی هیدروکربن‌های حلقوی به صورت مصنوعی بر اساس پساب صنعتی واقعی در غلظت‌های ۵۰، ۱۰۰ و ۱۵۰ میلی‌گرم در لیتر با استفاده از کاتالیزورهای MCM-41، در دوزهای ۰/۱، ۰/۵ و ۱ گرم، در مقادیر مختلف pH تهیه شد. در مطالعه حاضر، نتایج بهینه به دست آمده از روش تاگوچی، pH=11، به مدت ۶۰ دقیقه، غلظت محلول هیدروکربنی حلقوی BTEXS 100 میلی‌گرم در لیتر و دوز نانوذره ۰/۵ گرم بود. حداکثر حذف BTEXS ۷۷/۳۶ درصد با استفاده از پراکسید هیدروژن به دست آمد.